



**HAL**  
open science

# Effect of preparation on the commensurabilities and thermal expansion of graphene on Ir(111) between 10 and 1300 K

Fabien Jean, Tao Zhou, Nils Blanc, Roberto Felici, Johann Coraux, Gilles Renaud

► **To cite this version:**

Fabien Jean, Tao Zhou, Nils Blanc, Roberto Felici, Johann Coraux, et al.. Effect of preparation on the commensurabilities and thermal expansion of graphene on Ir(111) between 10 and 1300 K. *Physical Review B: Condensed Matter and Materials Physics (1998-2015)*, 2013, 88 (16), pp.165406. 10.1103/PhysRevB.88.165406 . hal-02014369

**HAL Id: hal-02014369**

**<https://hal.science/hal-02014369>**

Submitted on 11 Mar 2019

**HAL** is a multi-disciplinary open access archive for the deposit and dissemination of scientific research documents, whether they are published or not. The documents may come from teaching and research institutions in France or abroad, or from public or private research centers.

L'archive ouverte pluridisciplinaire **HAL**, est destinée au dépôt et à la diffusion de documents scientifiques de niveau recherche, publiés ou non, émanant des établissements d'enseignement et de recherche français ou étrangers, des laboratoires publics ou privés.

# Effect of preparation on the commensurabilities and thermal expansion of graphene on Ir(111) between 10 and 1300 K

Fabien Jean,<sup>1</sup> Tao Zhou,<sup>2</sup> Nils Blanc,<sup>1</sup> Roberto Felici,<sup>3</sup> Johann Coraux,<sup>1</sup> and Gilles Renaud<sup>2</sup>

<sup>1</sup>Univ. Grenoble Alpes, Inst NEEL, F-38042 Grenoble, France CNRS, Inst NEEL, F-38042 Grenoble, France

<sup>2</sup>Departement de Recherche Fondamentale sur la Matière Condensée/Service de Physique des Matériaux et des Microstructures, Commissariat à l'Energie Atomique Grenoble, 38054 Grenoble Cedex 09, France

<sup>3</sup>European Synchrotron Radiation Facility, BP 220, F-38043 Grenoble Cedex 9, France

The effects of the temperature on the structure of a single layer of graphene on Ir(111) have been investigated *in situ* in the growth chamber by grazing incidence x-ray diffraction between 10 and 1300 K. In addition, the effect of two growth temperatures has been studied. The graphene lattice parameter of the main, nonrotated phase displays a characteristic hysteresis whose lower and upper branches correspond to phases in which integer numbers  $(m,n)_{\text{Ir}}$  of the Ir lattice parameters match integer numbers  $(p,q)_{\text{Gr}}$  of the graphene lattice parameters, i.e., commensurate phases,  $(19,0)_{\text{Ir}} \times (21,0)_{\text{Gr}}$  and  $(9,0)_{\text{Ir}} \times (10,0)_{\text{Gr}}$ , respectively. With a higher growth temperature, graphene presents, in addition to a main nonrotated, incommensurate phase, domains with a small rotation ( $2.37^\circ$ ) relative to the substrate, corresponding to a  $(7,2)_{\text{Ir}} \times (8,2)_{\text{Gr}}$  commensurate phase. Despite the weak interaction between graphene and iridium, the thermal expansion coefficient of graphene is positive at all temperatures, even at liquid helium temperature contrary to free-standing graphene. It is also close to the iridium thermal expansion because of the tendency to form commensurate phases, which creates a strong link between the graphene and substrate lattices and decreases the elastic energy.

DOI: [10.1103/PhysRevB.88.165406](https://doi.org/10.1103/PhysRevB.88.165406)

PACS number(s): 61.48.Gh, 65.80.Ck, 68.65.Pq, 61.72.Dd

## I. INTRODUCTION

Two-dimensional (2D) crystals hold promise for future applications in nanotechnology.<sup>1</sup> Their most famous representative, graphene, has attracted a lot of attention due to its exceptional properties.<sup>2</sup>

Graphite's negative thermal expansion coefficient (TEC) below 500 K (Refs. 3 and 4) has been known for a long time. Graphene, a single layer of graphite, has been predicted to exhibit negative TEC as well, below 300 K, with a unique dependence of its lattice parameter with temperature due to the out-of-plane vibration modes that its membranelike topography allows.<sup>4,5</sup> This prediction was tested on both suspended graphene, in electromechanical resonators,<sup>6</sup> and on supported graphene, for graphene exfoliated from graphite and transferred to SiO<sub>2</sub>/Si.<sup>7</sup> The loose contact between graphene and SiO<sub>2</sub> (Ref. 8) presumably explains why graphene does not follow the TEC of the support. Which TEC graphene exhibits under the influence of a support with which it forms a good contact is of fundamental interest and an open question in any future application operating at variable temperature. The answer to this question is indeed, as we shall see, related to the formation of defects and strain, which are both known to modify the properties of graphene.<sup>9</sup>

Graphene grown on a metallic substrate is well suited to address this issue. Depending on the strength of the graphenemetal interaction, various situations have been reported. In graphene on Ru(0001), a prototypical system for a strong interaction (characterized by hybridizations between the metal and graphene electronic bands and charge transfers of the order of 1 eV), the TEC of graphene remains unknown. However a compressive strain larger than 1%, was found at room

temperature,<sup>10</sup> presumably resulting from the compression of the carbon lattice when cooling down from the growth temperature at which graphene locks in a commensurate phase on the Ru(0001) lattice. Graphene on Ir(111) exhibits contrasting properties, which can be traced back to the weak interaction between graphene and iridium (marginal hybridization of electronic bands between the two materials and typically 100-meV charge transfer<sup>11</sup>): its structure has low strain at room temperature,<sup>12</sup> which is ascribed to the partial relief of compressive strain by delaminating graphene, in the form of so-called wrinkles.<sup>13,14</sup> We note that this stress relief pathway is forbidden in graphene on Ru(0001) due to the strong C-Ru bonds.<sup>15</sup>

In this paper, we show that besides forming wrinkles, graphene can develop small rotations allowing it, or part of it in the form of domains, to lock in commensurate phases on Ir, during cooldown from the growth temperature. These in-plane rotations about the crystallographic orientation corresponding to zigzag carbon rows aligned to the dense-packed rows of Ir (referred to as  $R0^\circ$  in the following) are much smaller than those observed recently.<sup>16,17</sup> We also show that the  $R0^\circ$  orientation can be strained to a large extent, thus exploring a broad range of graphene-Ir(111) epitaxy between two different commensurate phases, which are stabilized over wide temperature ranges. We establish that the growth conditions influence the structure of graphene. Finally, whatever the preparation procedure, graphene is found to adopt a positive TEC on Ir(111) in the whole range of temperature between 10 and 1300 K.

The article is organized as follows. First, we describe the experimental methods. Results are represented in the next section

and discussed in the following one, before a last section devoted to conclusions and perspectives.

## II. METHODS

The synchrotron x-ray diffraction measurements were performed in ultrahigh vacuum chambers coupled with z axis diffractometers at the ID03 and BM32 beamlines of the European Synchrotron Radiation Facility (Grenoble, France). The base pressure of the chambers was below  $10^{-9}$  mbar. The grazing incidence x-ray diffraction (GIXD) measurements were conducted with monochromatic photon beams of 11 and 21 keV, with the incident angles, respectively, 0.21 and 0.19°, well below the critical angle for total external reflection, in order to keep the bulk background scattering as small as possible. The beam was focused to a size of  $35 \times 80 \mu\text{m}^2$  [full width at half-maximum (FWHM) in horizontal and vertical directions, respectively] at ID03 and  $300 \times 200 \mu\text{m}^2$  at BM32. In both cases, a 2D pixel detector (Maxipix) was positioned 570 mm (ID03) and 680 mm (BM32) away from the sample, and detector slits were placed before the detector,  $\sim 200$  mm away from the sample and opened at 0.5 mm parallel to the sample surface. The reciprocal space scans of the scattered intensity presented below are all normalized to the intensity measured with a monitor placed before the sample.

The Ir single crystal, cut and polished on a (111) surface termination to within  $0.1^\circ$ , was bought from the Surface Preparation Laboratory. It was cleaned by cycling ion bombardment and high temperature annealing (1573 K). The bombardments were performed at room temperature with 1.3-kV  $\text{Ar}^+$  ions for about 1 h. Oxygen at a partial pressure of  $5 \times 10^{-7}$  mbar was introduced in the chamber for 10 minutes at 1273–1373 K in order to deplete the bulk crystal from residual carbon and to achieve a clean surface.

Between 450 and 750 K, the sample temperature was measured with a pyrometer with an uncertainty of 50 K. A second pyrometer was used between 750 and 1600 K, with the same uncertainty. Between 10 and 300 K, the temperature was measured with a platinum thermocouple welded on a helium-cooled copper finger in contact with the sample holder. The sample was heated by electron bombardment of its backside. Ten minutes were needed to achieve thermal stabilization after each temperature change.

Different preparations of graphene were performed following a well-established method, consisting of a temperature-programmed growth (TPG) step followed by chemical vapor deposition (CVD),<sup>18</sup> as shown in Fig. 1, but with different growth temperatures in unveiling the role of this parameter. The different sample preparation conditions are summarized in Table I. For the two preparations, P1 and P2, graphene was prepared by exposing the surface to ethylene at  $10^{-7}$  mbar

TABLE I. Temperature of the TPG and CVD steps during the graphene growth (respectively, steps B and C in Fig. 1), types of commensurability detected on the different samples during heating and cooling, and their corresponding temperature range, for the two preparation methods P1 and P2.

	$T_{\text{TPG}}$ (K)	$T_{\text{CVD}}$ (K)	Type of commensurability	Temperature range (K)
P1	1473	1273	$(19,0)_{\text{Ir}} \times (21,0)_{\text{Gr}}$ (heating)	4 to 600
	–	–		1073 to 738
P2	1573	1373	$(9,0)_{\text{Ir}} \times (10,0)_{\text{Gr}}$ (cooling)	4 to 800
	–	–	$(7,2)_{\text{Ir}} \times (8,2)_{\text{Gr}}$ (heating)	1300 to 473
			$(9,0)_{\text{Ir}} \times (10,0)_{\text{Gr}}$ (cooling)	

at room temperature for 5 min, where ethylene partially dehydrogenates into ethylidyne on the surface,<sup>19</sup> then flashing the temperature ( $T_{\text{TPG}}$ ) for 20 s, which is known to yield graphene islands. Then, the sample was cooled down by 200 K to  $T_{\text{CVD}}$  and exposed to an ethylene partial pressure of  $10^{-8}$  mbar for more than 10 min (10 min of ethylene exposure is known to yield almost >99% coverage of graphene) and kept at the same temperature without ethylene for another 10 min.

On both samples, the lattice parameter and relative crystallographic orientation of graphene and Ir(111) were studied by analyzing the scattered intensity in an in-plane cut of the reciprocal space with radial scans along the in-plane component  $Q_r$  of the momentum transfer and with azimuthal scans along the angle  $\omega$ , respectively. The intensity is maximal where the crystal truncation rods of Ir(111) and the diffraction rods of graphene intersect the plane (parallel to the sample surface) of reciprocal space under investigation. The moiré-like superstructure typical of the graphene on iridium system also has distinctive peaks in GIXD, which are not presented here because they are not relevant to the focus of this paper.

The Ir triangular surface crystallographic cell is defined by the vectors  $\mathbf{a}_{\text{Ir}}^S = \frac{1}{2}(\mathbf{a}_{\text{Ir}}^B - \mathbf{b}_{\text{Ir}}^B)$  and  $\mathbf{b}_{\text{Ir}}^S = \frac{1}{2}(-\mathbf{a}_{\text{Ir}}^B + \mathbf{b}_{\text{Ir}}^B)$  with the Ir bulk lattice parameter at room temperature  $a_{\text{Ir}}^B = b_{\text{Ir}}^B = 3.8392 \text{ \AA}$ .<sup>20</sup> The length of the Ir surface lattice parameter at room temperature is then  $a_{\text{Ir}}^S = b_{\text{Ir}}^S = 2.7147 \text{ \AA}$  and will be referred to as  $a_{\text{Ir}}$  in the rest of the article. The unit cell vectors of graphene,  $\mathbf{a}_{\text{Gr}}$  and  $\mathbf{b}_{\text{Gr}}$  have a room temperature modulus, calculated for an isolated layer, of  $a_{\text{Gr}} = b_{\text{Gr}} = 2.456 \text{ \AA}$ .<sup>5</sup> From the measured  $Q_r$  position of the Bragg peaks, one deduces the corresponding distance between crystallographic planes

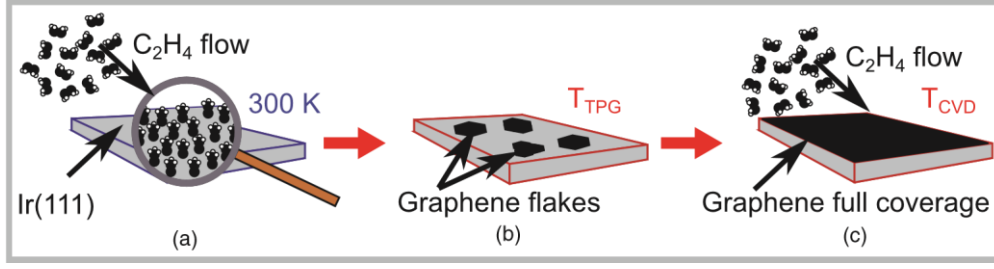


FIG. 1. (Color online) Sketch of the different steps of the TPG (a and b)+CVD (c) growth. The first step (a) is the adsorption of ethylene on the Ir(111) surface and its dehydrogenation as ethylidyne ( $-C_2H_3$ ) at room temperature. The second (b) is a flash at  $T_{TPG}$  without ethylene flow inside the chamber, resulting in the growth of graphene flakes. The graphene coverage at the end of this stage is  $\sim 20/25\%$ . The last step of the growth (c) is the completion of the graphene monolayer by CVD, with an ethylene flow and the sample at  $T_{CVD}$ . The coverage at the end is nearly  $>99\%$ .

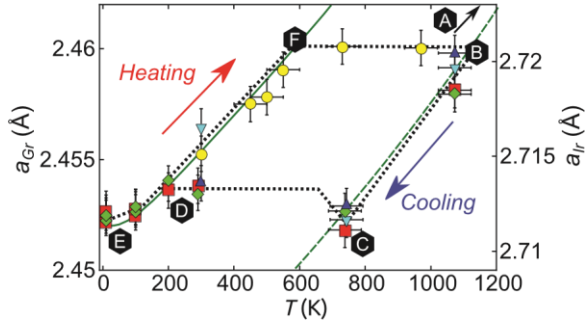


FIG. 2. (Color online) Evolution of the graphene lattice parameter  $a_{Gr}$  (left axis) of different samples prepared under the same conditions (P1), as a function of temperature ( $T$ ). Each color and shape corresponds to a different sample (blue upward pointing triangles, cyan downward pointing triangles, red squares, light green diamonds, and yellow circles). The dotted black line shows the shape of the hysteresis observed in Ref. 14. The solid green curve is the evolution of the bulk Ir lattice parameter (right axis) with temperature. The dashed green curve is the Ir green solid curve reported, as a guide for the eyes, to match the evolution of graphene lattice parameter at high temperature. The arrows and letters in the black hexagons mark specific steps of the thermal history of the samples. The growth is referred to as point A, and measurements began at the lower temperature on point B at 1073 K.

(perpendicular to the surface in the case studied here), thus the lattice parameter in graphene and Ir.

A commensurate phase between graphene and Ir(111) can be indexed by one vector of the unit cell of its coincidence lattice, i.e., by two pairs of integers  $(m,n)_{Ir}$  and  $(p,q)_{Gr}$  such that  $m \times \mathbf{a}_{Ir}^S + n \times \mathbf{b}_{Ir}^S = p \times \mathbf{a}_{Gr} + q \times \mathbf{b}_{Gr}$ . This relationship may be fulfilled at the expense of strains in graphene.

### III. RESULTS

Figure 2 shows  $a_{Gr}$  as a function of the sample temperature, measured through several experiments on different samples grown under the same condition (P1, to within 50 K of uncertainty on temperature measurements). For these measurements, the samples were cooled down to 10 K step by step. They were then reheated to 1300 K and cooled down again to 10 K

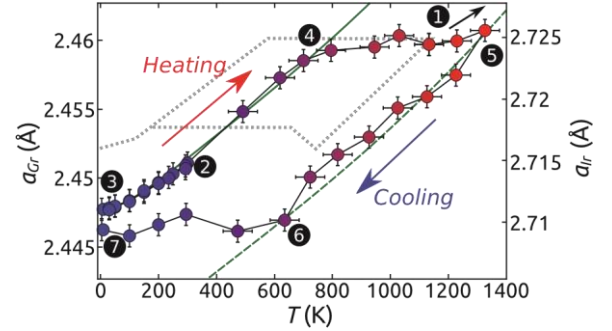


FIG. 3. (Color online) Evolution of the graphene lattice parameter  $a_{Gr}$  (left axis) for the second sample preparation (P2) as a function of the temperature ( $T$ ), as deduced from the radial location of the (110) reflection (blue and red circles). The solid green curve is the evolution of the bulk Ir lattice parameter (right axis) with temperature. The dashed green curve is the Ir green solid curve reported as a guide for the eyes to match the evolution of the graphene lattice parameter at high temperature. The arrows and numbers in the black circles mark specific steps of the thermal history of the sample. The growth is referred to as point A, and measurements began at the lower temperature on point B at 300 K.

before being finally reheated to room temperature. At each temperature, the Ir lattice parameter was deduced from the (110) and (020) Bragg reflections and is in accordance with the bulk thermal behavior.<sup>20</sup> The first observation is that graphene on Ir has a positive TEC over the whole temperature range, whatever the sample's history. The room temperature lattice parameter of graphene is found to be  $a_{Gr} = 2.4535 \pm 0.0008 \text{ \AA}$ . The lattice parameter, measured from 10 to 1100 K, displays a hysteresis, very similar to that reported by Hattab *et al.*<sup>14</sup> above room temperature and characteristic of the formation/removal of wrinkles in graphene. At the end of the growth, at about 1273 K (point A), graphene lies on its substrate without wrinkles. As the temperature is decreased, the graphene lattice parameter first follows the contraction of the Ir lattice (points B to C), leading to the buildup of compressive strain in graphene (relative to free-standing graphene at the same temperature). Wrinkles appear when further straining costs more energy than wrinkling, below  $\sim 800$  K (point C). From 800 K down to

The dotted gray lines shows the shape of the hysteresis observed in Ref. 14.

room temperature,  $a_{Gr}$  remains constant as the wrinkles keep growing (points C to D). Between 300 and 4 K (points D to E), the variation of the graphene lattice parameter follows that of Ir again, without new wrinkle formation. Graphene and Ir then follow the same behavior from the liquid helium temperature up to  $\sim 600$  K (points E to F). This implies that the wrinkles do not change, and graphene expands as much as its substrate. Above 600 K (points F to B),  $a_{Gr}$  remains constant, while the Ir substrate expands. At that point, the wrinkles begin to flatten, and the hysteresis loop closes when the growth temperature is reached. The transitions temperatures of  $\sim 800$  K (decreasing T) and  $\sim 600$  K (increasing T) are close to those (960 K and 650 K) reported in Ref. 14, for samples prepared in similar conditions.

Let us now follow the lattice parameter variations with temperature (Fig. 3) for the second sample preparation (P2). After preparation at 1373 K (point 1), the system has been cooled down to 300 K (point 2), where  $a_{Gr} = 2.4507 \pm 0.0008$  Å. Measurements were first performed during cooling down to 10 K and reheating to 300 K (points 2 to 3 and back to 2). The temperature was next increased to 1350 K (2 to 5) and cooled down to 10 K (5 to 7). As for P1, the graphene is found to have a positive TEC over the whole temperature range. Most importantly, as for P1, it has the same TEC as the Ir substrate between 3 and 4 and between 5 and 6, during heating and cooling, respectively. In addition, the graphene lattice parameter displays a hysteresis, which, unlike P1, is not fully closed: the lattice parameter is smaller after the sample has been heated to high temperatures. Indeed, the graphene lattice parameter at room temperature has decreased by 0.13% to  $a_{Gr} = 2.4474 \pm 0.0008$  Å. Moreover, the superposition of the hysteresis from Fig. 2 in dotted gray in Fig. 3 shows that P1 and P2 have different wrinkle nucleation temperatures.

Azimuthal scans close to the (020) reflection, as shown in Fig. 4, give more details about the epitaxial relationship

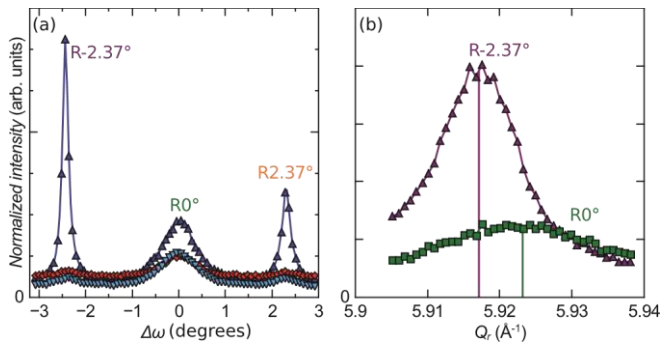


FIG. 4. (Color online) (a) Rocking scan of the graphene peaks on the (020) reflection of the first sample at 200 K before (blue upward pointing triangles) and after (cyan downward pointing triangles) high temperature annealing and at 945 K (red diamonds). The left (R-2.37° in purple) and right (R2.37° in orange) peaks on the curves are distant of  $-2.42^\circ$  and  $2.31^\circ$ , respectively, from the central peak ( $R0^\circ$  in green) at all temperature (T). (b) In-plane longitudinal scan of the left peak

(R-2.37°) in purple and central peak ( $R0^\circ$ ) in green from the blue curve in (a) at 200 K. Two lines show the position of the maximum of each peak. The intensities are normalized by the monitor and in linear scale.

of graphene with its substrate. Besides the peak at  $0^\circ$  corresponding to the contribution of the well-known  $R0^\circ$  phase, there are two narrower peaks, distant, respectively, of  $-2.42 \pm 0.01^\circ$  and  $+2.31 \pm 0.01^\circ$  from the central one (at

200 K on the first cooldown, in blue triangles). The fact that these peaks are not equally rotated from  $0^\circ$  is an artifact,<sup>21</sup> and the corresponding phase is referred to by the average orientation, as  $R2.37^\circ$  hereafter.

Radial scans in Fig. 4(b) show that the  $R2.37^\circ$  and  $R0^\circ$  phases do not have a maximum at the same  $Q_r$  (here, at 200 K) and thus have different lattice parameters. For  $R2.37^\circ$   $a_{Gr} = 2.4521 \pm 0.0008$  Å at 200 K, which is 0.08% larger than the lattice parameter of the  $R0^\circ$  domain at the same temperature. Moreover, the  $R2.37^\circ$  value does not vary with temperature. When heating from 300 K, the intensity of the side peak decreases significantly to become smaller than that of the  $R0^\circ$  peak above 795 K, as shown in Fig. 4. After cooling down to 200 K (cyan downward pointing triangles), the side peaks have almost vanished, and the intensity of the central peak has decreased by half. Moreover, the FWHM of the side peaks has increased markedly after the heating and cooling cycle, from  $\sim 0.21$  to  $0.48^\circ$ . By contrast, the FWHM of the  $R0^\circ$  peak is constant at  $0.8^\circ$  across the whole temperature loop. The intensity corresponding to the rotated domains has almost fully vanished at high temperature, where the first plateau of the hysteresis of the evolution of the graphene lattice parameter with temperature begins.

#### IV. DISCUSSION

As seen in Ref. 14 and for the sample preparation P1, the variation of  $a_{Gr}$  with temperature for the  $R0^\circ$  phase describes a hysteresis loop. Figure 5, in which  $a_{Gr}$  is normalized to  $a_{Ir}$ , shows that in addition, between the B and C points and between D and E, when graphene and iridium have the same behavior with temperature, nonrotated, commensurate phases are

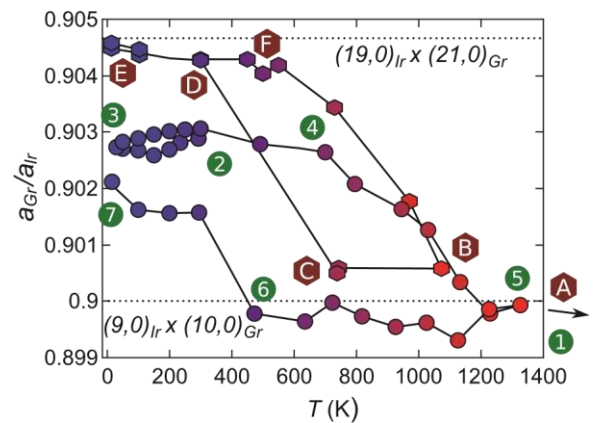


FIG. 5. (Color online) Ratio of the graphene and Ir lattice parameters  $a_{Gr}/a_{Ir}$  as a function of the temperature ( $T$ ). The P1 preparation is represented with red and blue diamonds and P2 with green and yellow circles. Black dotted lines signal commensurate ratios. The letters inside the brown hexagons (P1) and numbers inside the green circles (P2) denote specific steps of the thermal history of the samples.

stabilized. To a very good approximation, a  $(9,0)_{Ir} \times (10,0)_{Gr}$  commensurate phase is found at high temperature between B and C and a  $(19,0)_{Ir} \times (21,0)_{Gr}$  one at low temperature between D and E. The slight deviations from the  $a_{Gr}/a_{Ir}$  expected for these phases can be explained due to the coexistence of a small fraction of incommensurate phases. In Ref. 12, the incommensurate phases were found to dominate over commensurate ones. We interpret this difference as the consequence of different preparation conditions: for minimizing its elastic energy, graphene adopts different epitaxial relationships with its substrate at different growth temperatures, and the relief of elastic energy upon cooldown by wrinkle formation is only partial; in other words, graphene partly inherits its room temperature lattice from that at growth temperature.

For the sample preparation P2, two rotated phases with small rotations,  $2.37^\circ$  and  $-2.37^\circ$ , are present in addition to the nonrotated one. The influence of the growth temperature over the appearance of rotated phases on Ir(111) is a wellknown phenomenon.<sup>16,22</sup> These two rotated phases appear at the highest growth temperature and are quenched by the relatively fast cooldown to room temperature. However, their disappearance during the heating to high temperature shows that they are metastable. The observed irreversible loss of intensity of the  $R_{2.37^\circ}$  phase coincides with the temperature range in which wrinkles disappear. This corresponds to a regime where graphene is stretched by its substrate, which could result in the partial conversion of the  $R_{2.37^\circ}$  phase into other phases, either characterized by rather small size domains (well below the coherence length of the x-ray beam), having smaller in-plane rotations with respect to the Ir lattice or the main  $R_0^\circ$  phase.

The  $R_{2.37^\circ}$  phase is a commensurate one. Indeed, Fig. 6 shows that the  $R_{2.37^\circ}$  has a structure which matches a  $(7,2)_{Ir} \times (8,2)_{Gr}$  commensurate phase. This phase is characterized by a tensile strain (with respect to free-standing graphene) of 0.38% at 200 K. The corresponding moire has a 2.24-nm<sup>2</sup> periodicity, thus slightly smaller than the usual moire period of

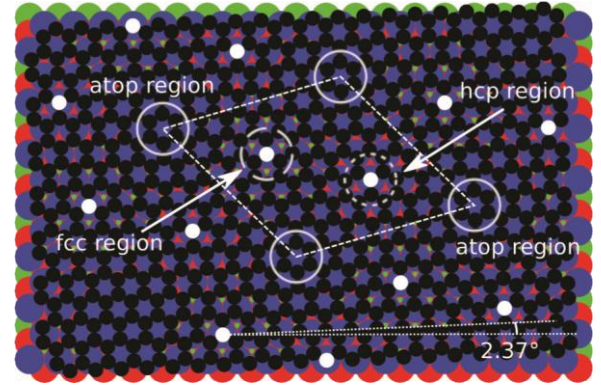


FIG. 6. (Color online) Sketch of the graphene on top of Ir(111) with a rotation of  $2.37^\circ$  as shown with the dotted white lines at the bottom (one is aligned with an Ir row and the other with a carbon row). Carbon atoms are shown as black disks, Ir atoms of the first, second, and third top layers are, respectively as blue, red, and green disks. Carbon atoms on top of Ir ones are shown as white disks. The new superlattice is highlighted with the dashed white frame. In the top regions (white circles in the corners of the cell), an Ir atom of the first layer is centered below a graphene hexagon. In the fcc region (dashed circle) and the hcp region (dotted circle), there are threefold-coordinated hollow sites centered under the carbon ring's center: either an fcc site (fcc region) or an hcp site (hcp region).

$2.52 \pm 0.02$  nm measured at the same temperature for the  $R_0^\circ$  phase. These rotational domains provide a new perspective on the reason why, for preparation P2, the graphene's TEC follows that of the Ir over a wider temperature range. The  $R_{2.37^\circ}$  has a higher density of carbon atoms whose position coincide with that of the Ir ones than the  $(19,0)_{Ir} \times (21,0)_{Gr}$  phase of preparation P1, allowing the system to be heated at higher temperature before wrinkles start to be stretched out (after point 4). This is consistent in a first approximation with the O-lattice theory, which states that the phase with the highest density of coincident sites is the most stable.<sup>23</sup> At 1300 K, the temperature is beyond the point where all wrinkles are flattened according to Hattab *et al.*<sup>14</sup> Similar to the preparation P1, there is in this system a competition between two states of the graphene/Ir system: a fully commensurate state at the cost of creating rotational domains and/or strains and a nonrotated state, for which the strain is better relieved by the graphene being incommensurate and forming or eliminating wrinkles.

For the two sample preparations, upon cooling down, the graphene contraction as a function of temperature follows the Ir behavior from 1300 to 650 K. In this temperature range, the interaction with the substrate, though known to be weak,<sup>11</sup> is large enough to allow for increasing strain without forming wrinkles to release it. Figure 5 shows that the graphene here is close to being commensurate with its substrate, in a  $(9,0)_{Ir} \times (10,0)_{Gr}$  phase. The misfit for this commensurate phase is only 0.34%, almost the same as the misfit of the  $R_{2.37^\circ}$  rotational domains. Below 650 K, the lattice parameter stabilizes during the wrinkle formation and growth.

As summarized in Table I, the structure of graphene grown on Ir(111) can vary significantly due to changes in the growth procedure. For the first sample preparation (P1), with a growth

temperature of 1273 K, graphene presents a hysteresis loop with temperature, being close to commensurate with its substrate at high and low temperature, where it displays an expansion behavior similar to the substrate over limited temperature ranges, and being incommensurate in the average in between, where wrinkles are present. For the second sample preparation (P2), with a 100 K-higher growth temperature, graphene presents different commensurate phases, unrotated and rotated, with the  $(9,0)_{\text{Ir}} \times (10,0)_{\text{Gr}}$  and  $(7,2)_{\text{Ir}} \times (8,2)_{\text{Gr}}$  commensurabilities, respectively. Those phases are linked with the broader temperature range, where the graphene and the Ir TECs are identical, during expansion or contraction. This is further evidence that the commensurability of graphene on Ir can be tailored by the growth process.

## V. CONCLUSION

The TEC of graphene grown on Ir(111) remains positive at all temperatures, regardless of the growth preparation. This is true even below room temperature, between 10 and 300 K, where the graphene TEC always follows the Ir one, whatever the previous thermal history.

Graphene on Ir is a system presenting two competing tendencies with temperature: either tending to adopt commensurate phases with its substrate at low and high temperatures, despite the weak interaction, with different commensurabilities depending on the preparation conditions, or forming wrinkles. When commensurate phases are present, graphene and Ir have identical TECs, because of the strong link created by the commensurability. This gives insight into other graphene on metal systems, such as graphene on Ru(0001), where different commensurate phases have been observed with different growth parameters.

## ACKNOWLEDGMENTS

We thank Thomas Dufrane, Olivier Geaymond and the staff members of the ID03 and BM32 beamlines, the Agence Nationale de la Recherche for funding (Contract No. ANR2010-BLAN-1019-NMGEM), and the European Union for funding through Contract No. NMP3-SL-2010-246073 "GRENADA".

<sup>1</sup>K. S. Novoselov, V. I. Fal'ko, L. Colombo, P. R. Gellert, M. G. Schwab, and K. Kim, *Nature (London)* **490**, 192 (2012).

<sup>2</sup>A. K. Geim, *Science* **324**, 1530 (2009).

<sup>3</sup>J. Nelson and D. P. Riley, *Proc. Phys. Soc.* **57**, 477 (1945).

<sup>4</sup>N. Mounet and N. Marzari, *Phys. Rev. B* **71**, 205214 (2005).

<sup>5</sup>K. Zakharchenko, M. Katsnelson, and A. Fasolino, *Phys. Rev. Lett.* **102**, 046808 (2009).

<sup>6</sup>V. Singh, S. Sengupta, H. S. Solanki, R. Dhall, A. Allain, S. Dhara, P. Pant, and M. M. Deshmukh, *Nanotechnology* **21**, 165204 (2010).

<sup>7</sup>D. Yoon, Y.-W. Son, and H. Cheong, *Nano Lett.* **11**, 3227 (2011).

<sup>8</sup>V. Geringer, M. Liebmann, T. Echtermeyer, S. Runte, M. Schmidt, R. Ruckamp, M. C. Lemme, and M. Morgenstern, *Phys. Rev. Lett.* **102**, 076102 (2009).

<sup>9</sup>A. H. Castro Neto, F. Guinea, N. M. R. Peres, K. S. Novoselov, and A. K. Geim, *Rev. Mod. Phys.* **81**, 109 (2009).

<sup>10</sup>D. Martoccia, P. R. Willmott, T. Brugger, M. Bjorck, S. Gunther, C. M. Schlepütz, A. Cervellino, S. A. Pauli, B. D. Patterson, S. Marchini, J. Winterlin, W. Moritz, and T. Greber, *Phys. Rev. Lett.* **101**, 126102 (2008).

<sup>11</sup>I. Pletikoscic, M. Kralj, P. Pervan, R. Brako, J. Coraux, A. T. N'Diaye, C. Busse, and T. Michely, *Phys. Rev. Lett.* **102**, 056808 (2009). <sup>12</sup>N. Blanc, J. Coraux, C. Vo-Van, A. T. N'Diaye, O. Geaymond, and G. Renaud, *Phys. Rev. B* **86**, 235439 (2012). <sup>13</sup>A. T. N'Diaye, J. Coraux, T. N. Plasa, C. Busse, and T. Michely, *New J. Phys.* **10**, 043033 (2008).

<sup>14</sup>H. Hattab, A. T. N'Diaye, D. Wall, C. Klein, G. Jnawali, J. Coraux, C. Busse, R. van Gastel, B. Poelsema, T. Michely, F.-J. M. zu Heringdorf, and M. Horn-von Hoegen, *Nano Lett.* **12**, 678 (2012).

<sup>15</sup>P. Sutter, P. Albrecht, X. Tong, and E. Sutter, *J. Phys. Chem. C* **117**, 6320 (2013).

<sup>16</sup>E. Loginova, S. Nie, K. Thurmer, N. Bartelt, and K. McCarty, *Phys. Rev. B* **80**, 085430 (2009).

<sup>17</sup>L. Meng, R. Wu, L. Zhang, L. Li, S. Du, Y. Wang, and H.-J. Gao, *J. Phys.: Condens. Matter* **24**, 314214 (2012).

<sup>18</sup>A. T. N'Diaye, S. Bleikamp, P. Feibelman, and T. Michely, *Phys. Rev. Lett.* **97**, 215501 (2006).

<sup>19</sup>T. S. Marinova and K. L. Kostov, *Surf. Sci.* **181**, 573 (1987).

<sup>20</sup>J. W. Arblaster, *Platinum Met. Rev.* **54**, 93 (2010).

<sup>21</sup>The measured intensity is the integration of the scattered signal across the gap of the detector slits, which are inclined with respect to the scattering vector. The measured azimuthal angles are thus the result of a projection, along this inclined direction, of the actual contribution, which corresponds to a  $\pm(2.42-2.31)/2 = 2.37^\circ$  azimuthal angle.

<sup>22</sup>H. Hattab, A. T. N'Diaye, D. Wall, G. Jnawali, J. Coraux, C. Busse, R. van Gastel, B. Poelsema, T. Michely, F.-J. Meyer zu Heringdorf, and M. Horn-von Hoegen, *Appl. Phys. Lett.* **98**, 141903 (2011). <sup>23</sup>W. Bollmann and H.-U. Nissen, *Acta Cryst. A* **24**, 546 (1968).